



Chapman-Kolmogorov Equations for a Complete Set of Distinct Reliability States of an Object

Paweł SZCZEPAŃSKI^{1*}, Józef ŻUREK²

¹*Military University of Technology, Faculty of Mechatronics and Aerospace,
2 gen. Witolda Urbanowicza Str., 00-908 Warsaw, Poland*

²*Air Force Institute of Technology
6 Księcia Bolesława Str., 01-494 Warsaw, Poland
Corresponding author's e-mail address: paszczep@wp.pl*

Received by the editorial staff on 5 October 2017

The reviewed and verified version was received on 14 December 2018

DOI 10.5604/01.3001.0012.7332

Abstract. The Chapman-Kolmogorov equations indicated in the title are a pretext to demonstrate a mathematically unrecognised truth about the effect of the reliability states of elements (which are generally understood as “subjects”) on the reliability states of a complete set of the same elements, which is called an object. Of importance here are not just the reliability characteristics of individual elements, but the independencies, dependencies and interdependencies between the elements. The relations were described in the language of graph theory. The availability matrix of the language of graph theory was translated to determine the size and probabilities of distinct reliability states of the object, the derivatives of their similarities, and the transition rates adequate to those derivatives. This article continues the research work which identifies the relationship of the properties of a complete set of distinct reliability states of an object with a widely understood theory of systems. The previous papers referred, among others, to: risk, safety, structure entropy, the reliability of the results of checks, and – most of all – technical diagnostics, both in the area of its algorithms and of its optimisation.

The object's serial reliability structure was not assumed in any of those papers, recognising that it would be a serious abuse. The research results were referred to all possible structures of a three-element object. It is believed that by virtue of the block diagrams appropriate to those structures, the readers hereof are provided with a realistic opportunity to practically (and inexpensively) verify the ideas presented here.

Keywords: Chapman-Kolmogorov equations, digraph, complete set, distinct reliability states, transition intensity

1. BACKGROUND

This article is another paper which indicates the relationship of the properties of a *complete set of distinct reliability states*¹ of an object [19, 32] with a widely understood theory of systems. The previous papers referred, among others, to: risk [17, 21], safety [17], structure entropy [18, 20], reliability of the results of checks [15] and – most of all – technical diagnostics, both in the area of its algorithms [23, 24] and of its optimisation [16]. The object's *serial reliability structure* was not assumed in any of those papers, and the reason for this is explained in [15, 22].

Chapman-Kolmogorov equations are long-established tools for process modelling. They are nearly always used to determine the probability of states m with identified mutual transitions of the states. This is evident in [1, 2, 3, 28]. Here, however, the application of Chapman-Kolmogorov equations was different. An attempt was made to determine *transition rate* λ for the transitions into the *probabilities of states* $r(m)$ by applying known dependencies. The dependencies are a result of not only the probabilistic characteristics of elements, but also their *dependence* and *independence*. Aside from the determination of derivatives in relation to time, time-relative determination of any other variable² was made possible.

A natural property of the probabilities of states in their complete set (and irrespective of the mathematical form of the probabilities) is a sum equal to one. This characteristic needed not to be assumed herein; however, a proper check was made for the sake of calculation reliability. A certain pattern existed for the total of the probability derivatives. That total was always zero.

The only (intuitively and practically understood) transitions sought here were those from the operational³ state of all elements to the states resulting from distinct combinations of non-operation of the elements.

An example form of a graph which illustrates the rule for three independent elements (see Fig. 1(a)) is shown in Fig. 1(b).

¹ The concept of “set of diagnostic states” in this paper is synonymous with “set of reliability states”, which may include “non-operational states”, “partial (reduced) operational states”, and “operational states”. The reference literature terms the concept of “set of reliability states” as a “set of object's malfunction states”.

² In a generic case, transition rates may depend on time, distance, number of cycles, shots fired, engine running hours, and other similar measures.

³ This term does not apply to the operational state of an object, but all of the object's elements. No equivalence between the terms should be sought, unless a single-output object is involved.

Determination of the size of a set of distinct reliability states of an object (card M^R) will be a subject of further and detailed consideration; however, given a two-valued assessment of the reliability states of elements e_i and the independence of the elements (as shown in Fig. 1(a)):

$$\text{card } M^R = \text{card } M^M = 2^n \tag{1}$$

with: M^M – set of possible reliability states; n – size of the elements.

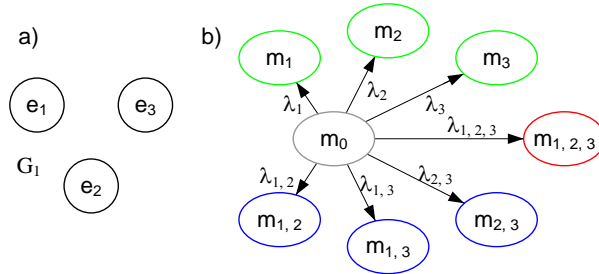


Fig. 1. Digraph G_1 of a selected structure of the object (Fig. 1(a)) and the graph of the object's distinct reliability states (Fig. 1(b)), with e_i being the i^{th} element of the object

If there was a single curve on digraph G tantamount to the presence of any dependence (or interdependence) between the elements:

$$\text{card } M^R < \text{card } M^M \tag{2}$$

The assumed direction of state transition allowed indexing the state transition rate λ with sets of non-operational elements: E_{nz} . The same rule applied to the indexing of states m and their respective probabilities r . Further on, the circles and the ellipses which symbolised the respective elements and states, the following denotations were omitted: e and m . While both terms denote directed graphs in the context hereof, the digraph applied to the structure of the object and graph meant the transitions from state m_0 to non-operational states $m_{E_{nz}}$. With the given order and according to the concept of Chapman-Kolmogorov equations:

$$\lambda_{E_{nz}} = \frac{r'_{E_{nz}}}{r_0} \tag{3}$$

whereas:

$$\lambda_0 = -\sum_{E_{nz}} \frac{r'_{E_{nz}}}{r_0} = \frac{r'_0}{r_0} \tag{4}$$

The total of transition rates for a full set of distinct reliability states was:

$$\lambda_0 + \sum_{E_{nz}} \lambda_{E_{nz}} = 0 \quad (5)$$

The validity of dependencies (3), (4) and (5) is shown in Table 1.

2. OBJECT DESCRIPTION WITH THE LANGUAGE OF GRAPH THEORY

For the sake of clarity of the analyses discussed herein, the authors chose to analyse all of the possible structures of a three-element object. An assumption for testing each of the structures individually was that the individual elements had only one output⁴. The number of inputs⁵ of any element was unlimited; the inputs for which it was certain they would accept input signals were omitted in the analyses.

An element was qualified as non-operational if its input signals were acceptable and the output signal was unacceptable. If present, any unacceptable input signal made the output signal of an element unacceptable and overrode that element's reliability state.

All technical objects could serve as examples that the foregoing assumptions were valid. A leading example of the analyses was an object whose G_2 digraph is shown in Fig. 2. The graph peaks (expressed with circles⁶) denote elements; the curves denote the directions of interaction of the elements.

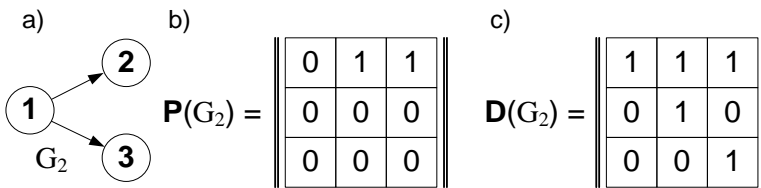


Fig. 2. Illustration of an object description with the language of graph theory: (a) digraph G_2 (the object's model); (b) and (c) binary matrices of: transitions $\mathbf{P}(G_2)$ and availability $\mathbf{D}(G_2)$

The binary matrix of transitions $\mathbf{P}(G_x)$ (Fig. 2(b)) was a mathematical description of the structure of digraph G_x . The Y and X-coordinates of the ones in the individual rows and columns denoted the direct successors and predecessors of the individual peaks.

⁴ All multi-output elements could be described with a structure of connections between single-output elements.

⁵ These inputs qualified the individual input signals as acceptable or unacceptable.

⁶ Peaks expressed with ellipses show reliability states.

In the binary matrix of availability $\mathbf{D}(G_x)$ (Fig. 2(c)), the ones in the rows and columns denoted all (direct and indirect) successors and predecessors of the individual peaks in digraph G_x . The sets of the successors and predecessors were termed respectively as follows in the language of graph theory: transitive closures $\widehat{F}(e_i)$ and anti-transitive closures $\widetilde{F}(e_i)$ [13]. For example, given digraph G_2 :

$$\widehat{F}(e_1) = \{e_1, e_2, e_3\} \tag{6}$$

whereas:

$$\widetilde{F}(e_3) = \{e_3, e_1\} \tag{7}$$

In a formal expression, the availability matrix was:

$$\mathbf{D}(G_x) = \sum_{k=0}^{n-1} \mathbf{P}^k(G_x) ; n = \text{card } E \tag{8}$$

with: E – set of digraph peaks. The totals and the multiplications denoted alternatives and conjunctions, respectively.

Matrix $\mathbf{D}(G_2)$ (Fig. 2(c)) assumed the form of an upper triangular matrix [7] by assignment of the numbering of the individual rows and columns which followed the sequential numbering of peaks in the successive layers of digraph G_2 [8]. Layer one included peaks without predecessors. Layer two included peaks which would not have any predecessors with the layer one peaks removed from the digraph. Layer three and each successive layer included the peaks which would not have any predecessors with the preceding layers removed from the digraph. Digraph G_2 (Fig. 1(a)) featured two layers:

$$W_1 = \{e_1\} \tag{9}$$

$$W_2 = \{e_2, e_3\} \tag{10}$$

Whether it was reasonable to apply an availability matrix depended on its computational complexity, a problem quite extensively discussed in a doctoral thesis [4]. Given this, multiple additional operations are usually due. At the stage of the graphical representation of a structure, all elements without measurement and control access were *aggregated*, while the elements of cycle C ; at $C > 1$ were *condensed*.

The condensation of peaks in cycle $C_i \min \subseteq E$ provided condensation (integration) of all peaks of the cycle into one peak, $e'_{i \min}$, with: i_{\min} – the lowest of all numbers of peaks. Aside from indexing the peak with the number, the peak was denoted with an apostrophe mark and a loop in its figure. When condensed, the graph was termed a Hertz's digraph and denoted G^H .

The condensation also reduced the scrutiny of diagnostic testing. The scrutiny could be increased if a non-operational state is proven to exist for element $e'_{i \min}$. This required physical splitting of cycle $C_{i \min}$ and insertion, at the split, of a signal identical to the signal from before the splitting.

The most spectacular operations were raising to a power the powers of triangular matrix $\mathbf{B} = \mathbf{P} + \mathbf{I}$, with: \mathbf{I} – a unit matrix [4, 8, 14]. The number of operations required was at least six times lower than raising the square matrix to a power. Matrix \mathbf{B} was iteratively raised to a power until the succeeding power equalled its direct predecessor. Currently, nearly all problems related to the determination and application of availability matrices are processed with dedicated computer software, which are discussed in [5, 6].

3. TRANSLATION OF THE AVAILABILITY MATRIX FOR THE DETERMINATION OF THE SIZE AND PROBABILITIES OF THE ELEMENTS IN A COMPLETE SET OF DISTINCT RELIABILITY STATES

The translation of the availability matrix for the determination of the size and probabilities of elements m in a complete set of distinct reliability states was, in essence, a translation for reliability diagnostics. The availability matrix described the diagnostic structure of a technical object; hence, the individual columns of the availability matrix could be assigned with checks, which were operations designed to test compliance of the output signals with their standards. If any of the parameters of a signal exceeded its limit, the check result was a failure. Otherwise, the check result was a pass. Both results had logical values assigned as 1 and 0.

The notation of the results of all checks, compliant with the numbering order of the latter, formed a binary row vector, in which the distribution of ones and zeros identified a specific reliability state⁷. If the distribution matched any of the rows in availability matrix $\mathbf{D}(G_x)$, the number of the row matched the number of a non-operational element. A mismatch would mean that [15]:

- all elements were operational (the vector contained zeros only);
- more than one element was non-operational;
- there were non-operational instances which mutually compensated themselves;
- failure of one or more results of individual checks.

The two latter options were not considered herein, as 100-percent reliability of the checks was assumed.

⁷ A reliability state, which in this context was one of the object states resulting from a certain combination of the reliability states of the object's elements; the paper did not use the following concepts (aside from "single-element object" and "single-output object"): "operational object" and "non-operational object".

Not unlike in the previous subsection, the consideration of the problem continued with reference to digraph G_2 , shown in Fig. 2(a). For this object (and any other object considered herein), only three checks were viable: s_1 , s_2 and s_3 . They were designed to test whether the output signals of the following elements were acceptable or not: e_1 , e_2 and e_3 . A certain pattern of testing the connection of the elements from digraph G_2 was that:

- the number of checks matched the number of individual non-operational instances;
- only one reliability state resulted when all elements were operational;
- only one reliability state was distinct as caused from more than one non-operational element; it was the state resulting from two non-operational elements, numbered with the coordinates of the single zero value instance to the right from the (main) diagonal of matrix $\mathbf{D}(G_2)$.

The latter question was depicted in Figs. 3(a) and 3(b), where the second one illustrated the result of totalling the rows with the designations of coordinates of that zero value.

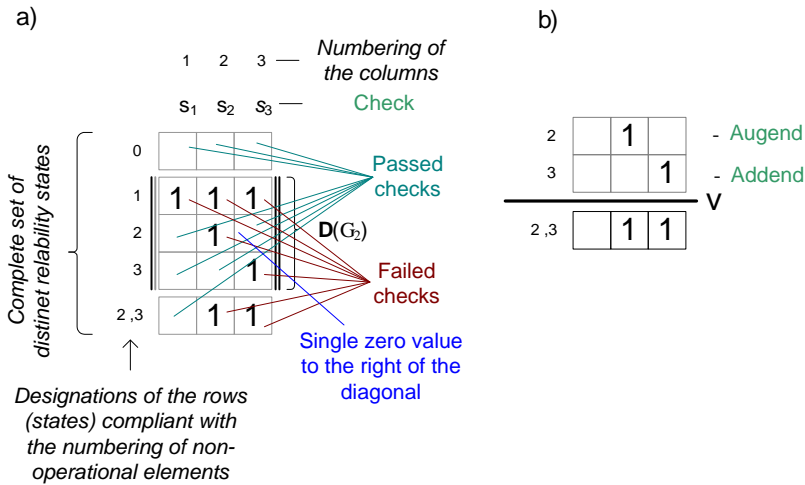


Fig. 3. Example of a translation of the availability matrix for the diagnosis of an object modelled with digraph G_2 : (a) determination of the complete set of distinct reliability states; (b) illustration of the determination of a binary representation of the reliability states of two elements identified with the numbering of the coordinates of the zero value to the right of the diagonal

The number of potential states M^M was 8, and the number of distinct states M^R was just 5. Note that when element e_1 was non-operational, it obscured the potential non-operational instances of elements e_2 and e_3 . The obscured non-operational instances could only be identified when the non-operational instance of element e_1 was removed (by restoring the element).

The next step of the investigation discussed here was to determine the probability of individual distinct reliability states. The probabilities depended on the diagnostic characteristics of the individual elements. The key to understanding the essence of this step was to understand the values of one of the diagonals in the upper triangular matrix $\mathbf{D}(G_x)$. The effort of identifying the state was reduced by determining the position of the first value of one to the left in the row vector of all results. The position matched the number of a non-operational element. Hence, if a row of matrix $\mathbf{D}(G_x)$ with a number of the same position had a distribution which matched the distribution of the results, the non-operational element identified was only a cause of the distribution. Each cause was denoted with an X, and (which should be understandable due to the identification with its position) the Y-coordinate of the character in matrix $\mathbf{D}(G_x)$.

The indication of the second X characters in those rows which represented the binary distributions of two distinct causes of non-operational instances required totalling the rows determined with the coordinates of the zero values located to the right of the diagonal. To fully represent its essence, the algorithm was best illustrated by reference to digraph G_1 (see Fig. 1(a)). In Fig. 4, the found zero values and the resulting totals were highlighted in orange.

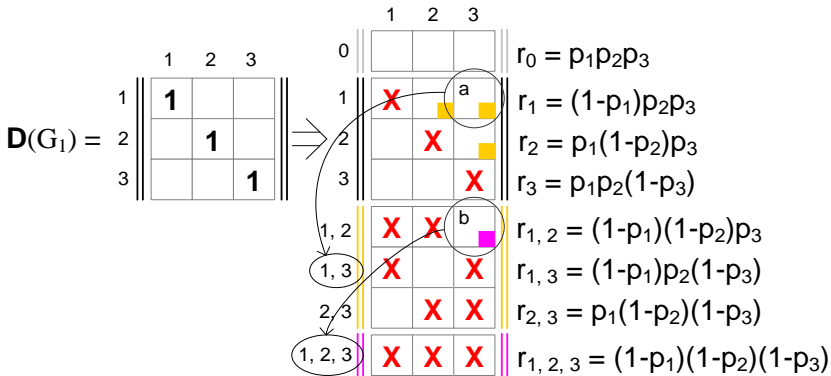


Fig. 4. Algorithm for the determination of the complete set of distinct reliability states

The process was iterative, with a different colour to highlight the designations in each iteration. The zero values which indicated it was feasible to determine the successive distinct causes of non-operational instances of the object, were sought to the right of the X characters at the right-hand edge.

The X-coordinate of each augend was complemented with the Y-coordinate of the addend. The total number of components in individual rows was determined by the number of the X characters contained.

The following alternatives existed when totalling the rows and the selection of each depended on the value of the addend and the augend:

$$0 \vee \mathbf{X} = \mathbf{X} \tag{11}$$

$$0 \vee 1 = 1 \tag{12}$$

$$0 \vee 0 = 0 \tag{13}$$

$$1 \vee 0 = 1 \tag{14}$$

$$1 \vee 1 = 1 \tag{15}$$

$$\mathbf{X} \vee 0 = \mathbf{X} \tag{16}$$

The alternative was regulated by the commutative law; however, in order to underscore the difference between the augend and the addend (given the adopted sequence of calculations), it must be noted and stressed beforehand that these operations:

$$\mathbf{X} \vee 1 \tag{17}$$

$$\mathbf{X} \vee \mathbf{X} \tag{18}$$

$$1 \vee \mathbf{X} \tag{19}$$

could not occur.

The process of iterative totalling ended when all zero values to the right of the right-hand of the X characters at the right-hand edge were processed. Note that each addend was a row of matrix $\mathbf{D}(G_x)$. The last operation was to add above the upper triangular matrix $\mathbf{D}(G_x)$ a row full of zeros only, which symbolised all passed checks.

This formed a matrix the rows of which determined unique binary sequences assigned to the individual elements of *the complete set of distinct reliability states*. The X characters present in the binary sequences replaced the values of one of the diagonals in matrix $\mathbf{D}(G_1)$ (see Fig. 4). The assignment of the following values (respectively) to the X characters, the zero values and the values of one⁸: $1-p_k$, p_k and 1, facilitated an automatic determination of probability r_{Enz} ; k – the Y-coordinates of the X characters, the zero values and the values of one. Note that the values of one were left with their original values. The value of one symbolises the obscuration of the reliability state of element e_k , the alternative of its reliability states, and the total of probabilities $p_k+q_k=1$.

The total of the probabilities determined as above was always equal to one. This happened irrespective of digraph G_x , i.e. the number of its peaks and the structure of peak connections. Moreover to determine the value of the total, the probabilities could have any value, with any nature of their changes, and with *any interrelation*. In this paper, the probability values naturally assumed only the values in the interval of $\langle 0; 1 \rangle$.

⁸ Which do not occur in digraph G_1 where all peaks were bare.

4. CHAPMAN-KOLMOGOROV EQUATIONS OF THE RELIABILITY STATES OF THREE-ELEMENT OBJECTS

As indicated at the beginning of the paper, Chapman-Kolmogorov equations were determined for all reliability (diagnostic) structures of three elements of an object with the graph shown in Fig. 1(b) and the dependencies (3) and (4). The examples of the probabilities resulting from the operational state of all three elements of the object, and the derivatives adequate to the probabilities were expressed with these dependencies:

$$r_0 = \begin{cases} p_1 p_2 p_3 & (20^I) \\ p^3 & (20^{II}) \\ e^{-a_1 t} e^{-a_2 t} e^{-a_3 t} = e^{-(a_1+a_2+a_3)t} & (20^{III}) \\ e^{-3at} & (20^{IV}) \end{cases}$$

$$r'_0 = \frac{d r_0}{d y} = \begin{cases} p_2 p_3 \Rightarrow r_0 = p_1 p_2 p_3 \wedge y = p_1 & (21^{Ia}) \\ p_1 p_3 \Rightarrow r_0 = p_1 p_2 p_3 \wedge y = p_2 & (21^{Ib}) \\ p_1 p_2 \Rightarrow r_0 = p_1 p_2 p_3 \wedge y = p_3 & (21^{Ic}) \\ 3p^2 \Rightarrow r_0 = p^3 \wedge y = p & (21^{II}) \\ -(a_1 + a_2 + a_3) e^{-(a_1+a_2+a_3)t} \Rightarrow r_0 = e^{-(a_1+a_2+a_3)t} \wedge y = t & (21^{III}) \\ -3a e^{-3at} \Rightarrow r_0 = e^{-3at} \wedge y = t & (21^{IV}) \end{cases}$$

with: y and a – respectively, the selected derivative argument, and the failure rate invariable in time for a single element.

In theory, the size of the possible dependencies was indeed unlimited for this state. In practice, however, it was limited by the nature of the individual elements, the probabilities of which, p_i (and q_i), could be a result of not only an exponential distribution [29].

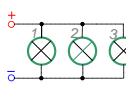
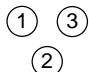
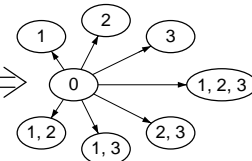


The cognitive process herein was focused on the individual structures of objects related to dependences ((20^{II}), (21^{II})) and ((20^{IV}), (21^{IV})). This facilitated a simple visualisation of transition rates λ_{Enz} (3) as a function of probability p and time t . The latter measure was assigned with a *conventional unit of time*: ujc , which an assumption was applied that:

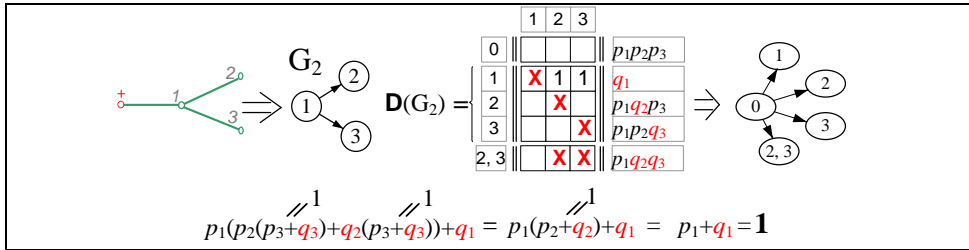
$$a = 1 \left[\frac{1}{ujc} \right] \quad (22)$$

Table 1 shows 9 object structures. Each structure was described with: a schematic diagram; digraph G_i ; availability matrix $D(G_i)$, with the potential distinct complements, which were determined with the algorithm shown in Fig. 4; the formulas of probabilities r_{Enz} for the distinct values of p_i and q_i ; a graph of transitions from state m_0 to distinct states m_{Enz} ; and a check whether the total of probabilities r_{Enz} was equal to 1.

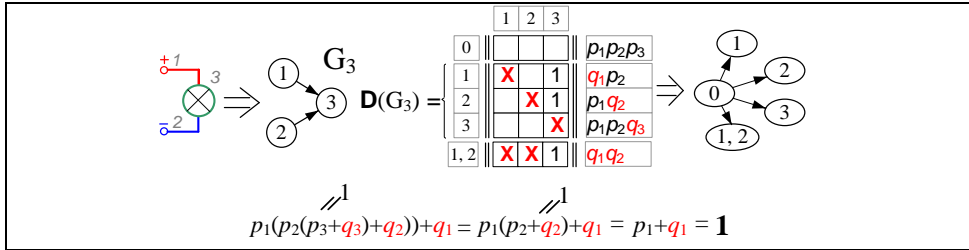
The further description of the structure was confined to two rows and four columns. Both rows contained the successive dependencies at r_{Enz} , r'_{Enz} , and λ_{Enz} . The dependencies in both rows were expressed for unified values of probabilities p_i and q_i , as well as $e^{-a_i t}$ and $1 - e^{-a_i t}$, which were equal to the following, respectively: p and $1-p$, as well as e^{-t} and $1 - e^{-t}$, if the value a (equal to a_i) was determined with formula (22). The fourth column (the first one from the right) should be treated as an annex to Table 1 with the plots shown in Fig. 5. Numbered colours were assigned to the individual equations and their plots. The results of the comparison between the equations referring to all of the 9 structures revealed certain identities, the sizes of which were expressed in Table 2 with suitable colours.

Table 1. Descriptions of individual structures of three-element objects (see the comments in the text)

  $D(G_1) = \begin{matrix} & \begin{matrix} 1 & 2 & 3 \end{matrix} \\ \begin{matrix} 0 \\ 1 \\ 2 \\ 3 \end{matrix} & \begin{bmatrix} & & & \\ \text{X} & & & \\ & \text{X} & & \\ & & \text{X} & \\ \text{X} & \text{X} & & \\ \text{X} & \text{X} & \text{X} & \\ & \text{X} & \text{X} & \\ \text{X} & \text{X} & \text{X} & \end{bmatrix} \end{matrix}$ 			
$p_1(p_2(p_3+q_3)+q_2(p_3+q_3))+q_1(p_2(p_3+q_3)+q_2(p_3+q_3)) = p_1(p_2+q_2)+q_1(p_2+q_2) = p_1+q_1 = \mathbf{1}$			
$r_0 = p^3$ $r_1 = r_2 = r_3 = (1-p)p^2$ $r_{1,2} = r_{1,3} = r_{2,3} = (1-p)^2p$ $r_{1,2,3} = (1-p)^3$	$r'_0 = 3p^2$ $r'_1 = r'_2 = r'_3 = 2p-3p^2$ $r'_{1,2} = r'_{1,3} = r'_{2,3} = 1-4p+3p^2$ $r'_{1,2,3} = -3+6p-3p^2$	$\lambda_0 = \frac{3}{p}$ $\lambda_1 = \lambda_2 = \lambda_3 = \frac{2-3p}{p^2}$ $\lambda_{1,2} = \lambda_{1,3} = \lambda_{2,3} = \frac{1-4p+3p^2}{p^3}$ $\lambda_{1,2,3} = \frac{-3+6p-3p^2}{p^3}$	
$r_0 = e^{-3t}$ $r_1 = r_2 = r_3 = (1-e^{-t})e^{-2t}$ $r_{1,2} = r_{1,3} = r_{2,3} = (1-e^{-t})^2e^{-t}$ $r_{1,2,3} = (1-e^{-t})^3$	$r'_0 = -3e^{-3t}$ $r'_1 = r'_2 = r'_3 = 3e^{-3t}-2e^{-2t}$ $r'_{1,2} = r'_{1,3} = r'_{2,3} = -e^{-t} + 4e^{-2t} - 3e^{-3t}$ $r'_{1,2,3} = 3e^{-t} - 6e^{-2t} + 3e^{-3t}$	$\lambda_0 = -3$ $\lambda_1 = \lambda_2 = \lambda_3 = 3 - 2e^t$ $\lambda_{1,2} = \lambda_{1,3} = \lambda_{2,3} = -e^{-t} + 4e^{-2t} - 3e^{-3t}$ $\lambda_{1,2,3} = 3e^{-t} - 6e^{-2t} + 3e^{-3t}$	



$r_0 = p^3$ $r_1 = 1-p$ $r_2 = r_3 = p^2(1-p)$ $r_{2,3} = (1-p)^2p$	$r'_0 = 3p^2$ $r'_1 = -1$ $r'_2 = r'_3 = 2p-3p^2$ $r'_{2,3} = 1-4p+3p^2$	$\lambda_0 = \frac{3}{p}$ $\lambda_1 = \frac{-1}{p^3}$ $\lambda_2 = \lambda_3 = \frac{2-3p}{p^2}$ $\lambda_{2,3} = \frac{1-4p+3p^2}{p^3}$	
$r_0 = e^{-3t}$ $r_1 = 1 - e^{-t}$ $r_2 = r_3 = (1 - e^{-t}) e^{-2t}$ $r_{2,3} = (1 - e^{-t})^2 e^{-t}$	$r'_0 = -3e^{-3t}$ $r'_1 = e^{-t}$ $r'_2 = r'_3 = 3e^{-3t} - 2e^{-2t}$ $r'_{2,3} = -e^{-t} + 4e^{-2t} - 3e^{-3t}$	$\lambda_0 = -3$ $\lambda_1 = e^{2t}$ $\lambda_2 = \lambda_3 = 3 - 2e^t$ $\lambda_{2,3} = -e^{2t} + 4e^t - 3$	



$r_0 = p^3$ $r_1 = r_2 = (1-p)p$ $r_3 = p^2(1-p)$ $r_{1,2} = (1-p)^2$	$r'_0 = 3p^2$ $r'_1 = r'_2 = 1 - 2p$ $r'_3 = 2p - 3p^2$ $r'_{1,2} = -2 + 2p$	$\lambda_3 = \frac{3}{p}$ $\lambda_1 = \lambda_2 = \frac{1-2p}{p^3}$ $\lambda_3 = \frac{2-3p}{p^2}$ $\lambda_{1,2} = \frac{-2+2p}{p^3}$	
$r_0 = e^{-3t}$ $r_1 = r_2 = (1 - e^{-t}) e^{-t}$ $r_3 = (1 - e^{-t}) e^{-2t}$ $r_{1,2} = (1 - e^{-t})^2$	$r'_0 = -3e^{-3t}$ $r'_1 = r'_2 = 2e^{-2t} - e^{-t}$ $r'_3 = 3e^{-3t} - 2e^{-2t}$ $r'_{1,2} = 2e^{-t} - 2e^{-2t}$	$\lambda_0 = -3$ $\lambda_1 = \lambda_2 = 2e^t - e^{2t}$ $\lambda_3 = 3 - 2e^t$ $\lambda_{1,2} = 2e^{2t} - 2e^t$	

<p style="text-align: center;">G₄</p> <p style="text-align: center;"> $\mathbf{D}(\mathbf{G}_4) = \begin{matrix} & \begin{matrix} 1 & 2 & 3 \end{matrix} \\ \begin{matrix} 0 \\ 1 \\ 2 \\ 3 \end{matrix} & \begin{bmatrix} & & \\ & \mathbf{X} & 1 & 1 \\ & & \mathbf{X} & 1 \\ & & & \mathbf{X} \end{bmatrix} \end{matrix}$ </p> <p style="text-align: center;"> $p_1(p_2(p_3+q_3)+q_2)+q_1 = p_1(p_2+q_2)+q_1 = p_1+q_1 = \mathbf{1}$ </p>			
$r_0 = p^3$ $r_1 = 1-p$ $r_2 = p(1-p)$ $r_3 = p^2(1-p)$	$r'_0 = 3p^2$ $r'_1 = -1$ $r'_2 = 1 - 2p$ $r'_3 = 2p - 3p^2$	$\lambda_0 = \frac{3}{p}$ $\lambda_1 = \frac{-1}{p^3}$ $\lambda_2 = \frac{1-2p}{p^3}$ $\lambda_3 = \frac{2-3p}{p^2}$	
$r_1 = e^{-3t}$ $r_1 = 1 - e^{-t}$ $r_2 = e^{-t}(1 - e^{-t})$ $r_3 = e^{-2t}(1 - e^{-t})$	$r'_0 = -3e^{-3t}$ $r'_1 = e^{-t}$ $r'_2 = 2e^{-2t} - e^{-t}$ $r'_3 = 3e^{-3t} - 2e^{-2t}$	$\lambda_0 = -3$ $\lambda_1 = e^{2t}$ $\lambda_2 = 2e^t - e^{2t}$ $\lambda_3 = 3 - 2e^t$	
<p style="text-align: center;">G₆</p> <p style="text-align: center;"> $\mathbf{D}(\mathbf{G}_6) = \begin{matrix} & \begin{matrix} 1 & 2 & 3 \end{matrix} \\ \begin{matrix} 1 \\ 2 \\ 3 \end{matrix} & \begin{bmatrix} 1 & & \\ & 1 & \\ & & 1 & 1 \\ & & & 1 & 1 \end{bmatrix} \end{matrix}$ </p> <p style="text-align: center;"> $\mathbf{D}(\mathbf{G}_6^H) = \begin{matrix} & \begin{matrix} 1 & 2' \end{matrix} \\ \begin{matrix} 0 \\ 1 \\ 2' \\ 1, 2' \end{matrix} & \begin{bmatrix} & \\ & \mathbf{X} & \\ & \mathbf{X} & \\ & \mathbf{X} & \mathbf{X} \end{bmatrix} \end{matrix}$ </p> <p style="text-align: center;"> $p_1(p_2+q_2)+q_1(p_2+q_2) = p_1+q_1 = \mathbf{1}$ </p>			
$r_0 = p^3$ $r_1 = (1-p)p^2$ $r_2 = (1-p^2)p$ $r_{1,2'} = (1-p^2)(1-p)$	$r'_0 = 3p^2$ $r'_1 = 2p-3p^2$ $r'_{2'} = 1-3p^2$ $r'_{1,2'} = -1-2p+3p^2$	$\lambda_0 = \frac{3}{p}$ $\lambda_1 = \frac{2-3p}{p^2}$ $\lambda_{2'} = \frac{1-3p^2}{p^3}$ $\lambda_{1,2'} = \frac{-1-2p+3p^2}{p^3}$	
$r_0 = e^{-3t}$ $r_1 = e^{-2t}(1 - e^{-t})$ $r_2 = e^{-t}(1 - e^{-2t})$ $r_{1,2'} = (1 - e^{-2t})(1 - e^{-t})$	$r'_0 = -3e^{-3t}$ $r'_1 = 3e^{-3t} - 2e^{-2t}$ $r'_{2'} = 3e^{-3t} - e^{-t}$ $r'_{1,2'} = e^{-t} + 2e^{-2t} - 3e^{-3t}$	$\lambda_0 = -3$ $\lambda_1 = 3 - 2e^t$ $\lambda_2 = 3 - e^{2t}$ $\lambda_{1,2'} = e^{2t} + 2e^t - 3$	

$p_1(p_2(p_3+q_3)+q_2)+q_1(p_2(p_3+q_3)+q_2) = p_1(p_2+q_2)+q_1(p_2+q_2) = p_1+q_1 = \mathbf{1}$			
$r_0 = p^3$ $r_1 = r_3 = (1-p)p^2$ $r_2 = (1-p)p$ $r_{1,2} = (1-p)^2$ $r_{1,3} = (1-p)^2p$	$r'_0 = 3p^2$ $r'_1 = r'_3 = 2p-3p^2$ $r'_2 = 1-2p$ $r'_{1,2} = -2+2p$ $r'_{1,3} = 1-4p+3p^2$	$\lambda_0 = \frac{3}{p}$ $\lambda_1 = \lambda_3 = \frac{2-3p}{p^2}$ $\lambda_2 = \frac{1-2p}{p^3}$ $\lambda_{1,2} = \frac{-2+2p}{p^3}$ $\lambda_{1,3} = \frac{1-4p+3p^2}{p^3}$	
$r_0 = e^{-3t}$ $r_1 = r_3 = e^{-2t}(1 - e^{-t})$ $r_2 = e^{-t}(1 - e^{-t})$ $r_{1,2} = (1 - e^{-t})^2$ $r_{1,3} = e^{-t}(1 - e^{-t})^2$	$r'_0 = -3e^{-3t}$ $r'_1 = r'_3 = 3e^{-3t} - 2e^{-2t}$ $r'_2 = 2e^{-2t} - e^{-t}$ $r'_{1,2} = 2e^{-t} - 2e^{-2t}$ $r'_{1,3} = -e^{-t} + 4e^{-2t} - 3e^{-3t}$	$\lambda_0 = -3$ $\lambda_1 = \lambda_3 = 3 - 2e^t$ $\lambda_2 = 2e^t - e^{2t}$ $\lambda_{1,2} = 2e^{2t} - 2e^t$ $\lambda_{1,3} = -e^{2t} + 4e^t - 3$	
$p_1p_2+q_1+p_1q_2 = p_1(p_2+q_2)+q_1 = p_1+q_1 = \mathbf{1}$			
$r_0 = p^3$ $r_1 = 1-p$ $r_{2'} = (1-p^2)p$	$r'_0 = 3p^2$ $r'_1 = -1$ $r'_{2'} = 1 - 3p^2$	$\lambda_0 = \frac{3}{p}$ $\lambda_1 = \frac{-1}{p^3}$ $\lambda_{2'} = \frac{1-3p^2}{p^3}$	
$r_0 = e^{-3t}$ $r_1 = 1 - e^{-t}$ $r_{2'} = (1 - e^{-2t})e^{-t}$	$r'_0 = 3e^{-3t}$ $r'_1 = e^{-t}$ $r'_{2'} = 3e^{-3t} - e^{-t}$	$\lambda_0 = -3$ $\lambda_1 = e^{2t}$ $\lambda_{2'} = 3 - e^{2t}$	

$p_1 p_3 + q_1 + p_1 q_3 = p_1 (p_3 + q_3) + q_1 = p_1 + q_1 = \mathbf{1}$			
$r_0 = p^3$ $r_{1'} = 1 - p^2$ $r_3 = (1 - p)p^2$	$r'_{0'} = 3p^2$ $r'_{1'} = -2p$ $r'_{3'} = 2p - 3p^2$	$\lambda_0 = \frac{3}{p}$ $\lambda_{1'} = \frac{-2}{p^2}$ $\lambda_{3'} = \frac{2 - 3p}{p^2}$	
$r_0 = e^{-3t}$ $r_{1'} = 1 - e^{-2t}$ $r_3 = (1 - e^{-t}) e^{-2t}$	$r'_{0'} = -3e^{-3t}$ $r'_{1'} = 2e^{-2t}$ $r'_{3'} = 3e^{-3t} - 2e^{-2t}$	$\lambda_0 = -3$ $\lambda_{1'} = 2e^t$ $\lambda_{3'} = 3 - 2e^t$	
$p_1 + q_1 = \mathbf{1}$			
$r_0 = p^3$ $r_{1'} = 1 - p^3$	$r'_{0'} = 3p^2$ $r'_{1'} = -3p^2$	$\lambda_0 = \frac{3}{p}$ $\lambda_{1'} = \frac{-3}{p}$	
$r_0 = e^{-3t}$ $r_{1'} = 1 - e^{-3t}$	$r'_{0'} = -3e^{-3t}$ $r'_{1'} = 3e^{-3t}$	$\lambda_0 = -3$ $\lambda_{1'} = 3$	

The proper interpretation of the plots was aided by the understanding of *the effect of overriding* certain reliability states by other reliability states, and the identification of *the size of non-operational elements* in those reliability states.

A study of the variations of r_{Enz} , r'_{Enz} and λ_{Enz} vs. time (see the right column in Fig. 5 and the bottom rows of the description of the individual structures in Table 1) provided the following conclusions:

$$\lambda_{E_{nz}}(t=0) = \begin{cases} 0 \Rightarrow \text{card } E_{nz} > 1 \\ 1 \Rightarrow \text{card } E_{nz} = 1 \\ \text{card } C \Rightarrow C \subseteq E_{nz} \\ -\text{card } E \Rightarrow E_{nz} = \emptyset \end{cases} \quad (23)$$

The increase in transition rate λ_{Enz} was primarily in the elements of the first layers w_1 of individual objects and the equations referring to the states identified with the colours 8, 3, 9, 7, and 6. The increase would speed up with the increase of the failure rate of the elements in those layers. This property was most evident in each cycle C as the size of the elements of the cycles increased. Here, an example of a cycle is a condensate: element e'_1 in digraph G_8 (see plot colour no. 8). The speed of the transition rate λ_{Enz} also depended on the range of effect from $e_i \in E_{\text{nz}}$ on all other elements of the same object.

Aside from element e'_1 , the highest effect was revealed for elements e_1 in digraphs G_2 , G_4 , and G_7 (see plot colour 3). The powers of the transitive closures of these elements were at their maximum.

The passage of time contributed to a drastic increase of the transition rates assigned to the states which resulted from multiple non-operational instances (see digraph G_1 and plot colour 6).

A study of transition rates $\lambda_{\text{Enz}}(p)$ revealed similar conclusions. To expose this, the variability of measures r_{Enz} , r'_{Enz} , and λ_{Enz} was visualised between the maximum and minimum values of probability p . An advantage of the analyses was the feasibility of including the whole range of variability of p : from 1 to 0. Transition rate $\lambda_0(t)$, analysed as a function of time, was constant and equal to the total (which here was triple the value) of failure rates of the object (see plot colours 10 and 11, and digraph G_9).

Consideration of the area of transition rate λ provided a clearer image of the object's properties. The derivatives (which were the measure of the function's value change rate relative to the changes of the function's arguments), when divided by probability r_0 , underwent very fast changes. As the probability approached zero, the transition rate values were spread asymptotically towards $\pm\infty$. This caused the authors hereof to limit the considerations to a range between $p = 1$ and $p = 0.6$ and a range between $t = 0$ and $t = 1.5\text{ujc}$ (see Fig. 5).

For a complete review, other forms of description should be mentioned. For example, for the digraph G_2 , the Chapman-Kolmogorov equation (according to Eq. (2) and (3)) takes a form of Eq. (24), which in fact is conversion of a well-known form of this system, determined by Eq. (25).

The paper presents the possibility of application, in addition to the time t , also the probability p , unified for all the object's elements. Indeed, in dependence on the object's nature, also the arguments can be cycles, road, working hours, number of shots, ... It depends, among others, on probability distributions of capability (incapability) of particular elements and on expression of the particular failure rates a .

If it has not been recognised yet, it should be pointed out that the failure rate a is not equivalent with the transition rate λ . An exception is a single-element, single-output object. And what will happen, if the distribution would be different than an exponential distribution? A reader will find the answer to this question in the last section of Chapter 3.

$$\left\{ \begin{array}{l} \lambda_0 = \frac{r'_0}{r_0} \\ \lambda_1 = \frac{r'_1}{r_0} \\ \lambda_2 = \frac{r'_2}{r_0} \\ \lambda_3 = \frac{r'_3}{r_0} \\ \lambda_{2,3} = \frac{r'_{2,3}}{r_0} \end{array} \right. \quad (24)$$

$$\left\{ \begin{array}{l} \frac{dr_0(t)}{dt} = \lambda_0 r_0(t) \\ \frac{dr_1(t)}{dt} = \lambda_1 r_0(t) \\ \frac{dr_2(t)}{dt} = \lambda_2 r_0(t) \\ \frac{dr_3(t)}{dt} = \lambda_3 r_0(t) \\ \frac{dr_{2,3}(t)}{dt} = \lambda_{2,3} r_0(t) \end{array} \right. \quad (25)$$

Because of a form of the digraph state and the known values r and r' , it should not be determined as a system of equation but, as it was pointed in the subject of the hitherto article, rather as equations.

In addition to the presented values λ and r (see Table 1), there are also known from the literature, their presentations expressed with matrices: rate matrix $\mathbf{\Lambda}$ and stochastic matrix \mathbf{S}^9 , that for the digraph G_2 and for the variable p have the form of Eq. (26) and Eq. (27), respectively.

$$\mathbf{\Lambda}(p) = \begin{array}{c} \begin{array}{c} 0 \\ 1 \\ 2 \\ 3 \\ 2,3 \end{array} \left\| \begin{array}{ccccc} & 0 & 1 & 2 & 3 & 2,3 \\ \hline \begin{array}{c} 3 \\ p \end{array} & \begin{array}{c} -1 \\ p^3 \end{array} & \begin{array}{c} 2-3p \\ p^2 \end{array} & \begin{array}{c} 2-3p \\ p^2 \end{array} & \begin{array}{c} 1-4p+3p^2 \\ p^3 \end{array} \\ \hline \begin{array}{c} 0 \\ 0 \end{array} & \begin{array}{c} 0 \\ 0 \end{array} & \begin{array}{c} 0 \\ 0 \end{array} & \begin{array}{c} 0 \\ 0 \end{array} & \begin{array}{c} 0 \\ 0 \end{array} \\ \hline \begin{array}{c} 0 \\ 0 \end{array} & \begin{array}{c} 0 \\ 0 \end{array} & \begin{array}{c} 0 \\ 0 \end{array} & \begin{array}{c} 0 \\ 0 \end{array} & \begin{array}{c} 0 \\ 0 \end{array} \\ \hline \begin{array}{c} 0 \\ 0 \end{array} & \begin{array}{c} 0 \\ 0 \end{array} & \begin{array}{c} 0 \\ 0 \end{array} & \begin{array}{c} 0 \\ 0 \end{array} & \begin{array}{c} 0 \\ 0 \end{array} \end{array} \right\| \end{array} \quad (26)$$

⁹ Common name of this matrix is the *transition* matrix \mathbf{P} . Here, this name and this indication are not used because they could be confused with (meaningfully different): binary matrix of *transitions* described in Chapter 2 (see Eq. (8)).

$$\mathbf{S}(p) = \begin{matrix} & \begin{matrix} 0 & 1 & 2 & 3 & 2,3 \end{matrix} \\ \begin{matrix} 0 \\ 1 \\ 2 \\ 3 \\ 2,3 \end{matrix} & \begin{vmatrix} p^3 & 1-p & p^2-p^3 & p^2-p^3 & p-2p^2+p^3 \\ 0 & 1 & 0 & 0 & 0 \\ 0 & 0 & 1 & 0 & 0 \\ 0 & 0 & 0 & 1 & 0 \\ 0 & 0 & 0 & 0 & 1 \end{vmatrix} \end{matrix} \quad (27)$$

The sums of terms of each row in the matrices \mathbf{A} and \mathbf{S} , are equal to 0 and 1, respectively. It should be remembered that the last sum results from application of the Chapman-Kolmogorov equations.

The matrices \mathbf{A} and \mathbf{S} belong to so-called sparse matrices in which most of the elements are zero. Such kind of a matrix is especially clear with respect to considered here double layer state digraphs. For example, for 100 states, a number of insignificant elements was 9900.

5. CONCLUSION

The contents of this paper can be a starting point for a wider analysis. The main objective of this paper was to indicate: the significance of the functional structure of an object to its probabilistic characteristics, and the realisation of the need to consider the probabilities of the operational instances of elements independent from non-operational elements. It is believed that an analysis of the properties of structurally distinct three-element objects exhausts the spectrum of the most important relations which may occur anywhere else. This may include a machine [32], an aircraft [9], a combat vehicle [11], an ICT system [12], a passenger vehicle [27], a radar [10], etc. Given the feasibility of building physical models of systems comprising electric batteries, light bulbs, wires, relays etc. electrical parts [16, 17, 25], simulating non-operational instances will not incur significant costs. An examples of proposals similar to the foregoing modelling is the testing of a circuit, comprising an electric motor, and described in [30, 31]. They found applications wherever serially connected elements exist. These investigations focused on the problem of identifying the reliability states caused by partial non-operational instances in individual elements.

A proof of the results presented herein could be an analysis of interactions with subjects in the direct environment of any human being, meaning their family, organisational structure [18], or practice in property management [26].

REFERENCES

- [1] Aalen Odd, Ornulf Borgan, Hakon Gjessing. 2008. Appendix A. Markov processes and the product-integral. In: *Survival and event history analysis. A process point of view*, 461-475. Springer.
- [2] Dawydow Pawel. 1988. *Technical diagnostics of electronic devices and systems* (in Russian). Moscow: Publishing House "Radio and communication".
- [3] Breuer Lothar. 2014. *Introduction to stochastic process*. Univ, Kent.
- [4] Dudziński Jacek, Paweł Szczepański. 1990. Rozprawa doktorska. Diagnostowanie złożonych obiektów technicznych z uszkodzeniami wielokrotnymi. Warszawa: Wydawnictwo WAT.
- [5] Fedyna Konrad, Paweł Szczepański 1993. Stanowisko komputerowej analizy i syntezy diagnostycznej złożonego obiektu technicznego. W *Materiały VII Krajowego Sympozjum Eksploatacji Urządzeń Technicznych. Problemy Eksploatacji 6/93. Diagnostyka*. 81-86. Radom-Kozubnik.
- [6] Fedyna Konrad, Ireneusz Machej, Paweł Szczepański. 1993. *Komputerowe stanowisko analizy i syntezy diagnostycznej złożonych obiektów technicznych. Instrukcja do ćwiczenia laboratoryjnego*. Warszawa: Wydawnictwo WAT.
- [7] Kaczorek Tadeusz. 1984. *Macierze w automatyce i elektrotechnice*. Warszawa: Wydawnictwo Naukowo-Techniczne.
- [8] Korzan Bohdan. 1978. *Elementy teorii grafów i sieci, Metody i zastosowania*. Warszawa: Wydawnictwo Naukowo-Techniczne.
- [9] Lewitowicz Jerzy, Kamila Kustroń. 2003. *Podstawy eksploatacji statków powietrznych – własności i właściwości eksploatacyjne statku powietrznego. T. 2*. Warszawa: Wydawnictwo ITWL.
- [10] Młokosiewicz Jerzy Ryszard. 1987. *Metoda wielopoziomowego badania stanu obiektów technicznych i synteza systemu diagnostycznego*. Warszawa: Wydawnictwo WAT.
- [11] Niziński Stanisław, Arkadiusz Rychlik. 2011. „Model diagnostyczny złożonego obiektu technicznego”. *Biuletyn WAT LX(1)* : 195-209.
- [12] Siergiejczyk Mirosław, Adam Rosiński. 2015. “Selected aspects of the supervision of ICT systems used in the rail transport”. *Diagnostyka* 16(2) : 62-67.
- [13] Sołowiew B. G. 1974. *Topological diagnostic model of objects with block structure. Diagnostics and identification* (in Russian). Riga: Zinatne.
- [14] Szczepański Paweł. 1985. „Propozycja metody lokalizacji uszkodzeń wielokrotnych w złożonych obiektach technicznych”. *Biuletyn WAT 7* : 93-101.

- [15] Szczepański Paweł. 2007. „Wiarygodność diagnozy”. *Pomiary-Automatyka-Robotyka (PAR)* 2, (CD).
- [16] Szczepański Paweł. 2012. Dynamic programming of full conditional program for diagnosing, *Diagnostyka – Applied structural health, usage and condition monitoring* 3(63) : 55-58.
- [17] Szczepański Paweł. 2014. „Para zagrożeniowo-ochronna jako element szacowania bezpieczeństwa obiektu i ryzyka”. *Biuletyn WAT* 63(4) : 233-257.
- [18] Szczepański Paweł, Janusz Płaczek. 2012. „Entropia struktur organizacyjnych przedsiębiorstw”. *Ekonomika i organizacja przedsiębiorstw* 3: 3-17.
- [19] Szczepański Paweł. 2001. „Określanie i zastosowanie prawdopodobieństw występowania rozróżnialnych stanów wadliwego funkcjonowania obiektu”. *Biuletyn WAT* 8 : 25-40.
- [20] Szczepański Paweł. 2009. „Entropia struktury obiektu w ujęciu addytywnym”. *Biuletyn WAT* LVIII(3) : 169-192.
- [21] Szczepański Paweł. 2009. „Ryzyko naprawy obiektu”. *Pomiary-Automatyka-Robotyka (PAR)* 2 (CD).
- [22] Szczepański Paweł. 2011. “Erroneous use of Bayes’ theorem in technical diagnostic”. *Diagnostyka – diagnostics and structural health monitoring* 1(57) : 47-54.
- [23] Szczepański Paweł, 1994. O wielokrokowości procesu diagnozowania złożonego obiektu technicznego. W *Materiały IX Konferencji Naukowo-Technicznej nt.: Diagnostyka maszyn roboczych i pojazdów*: 325-329.
- [24] Szczepański Paweł. 1997. „Wielotorowość w warunkowym programie diagnozowania złożonego obiektu technicznego”. *Biuletyn WAT* 2 : 111-122.
- [25] Szczepański Paweł. 2003. „Funkcjonalna struktura niezawodnościowa obiektu na przykładzie diagnozowania szeregowo połączonych elementów”. *Diagnostyka* 28 : 53-62.
- [26] Szczepański Paweł. 2011. Program badań diagnostycznych dla potrzeb gospodarowania nieruchomościami. W *Zagadnienia gospodarowania nieruchomościami*, 83-98. Warszawa: Wydawnictwo WSGN.
- [27] Tylicki Henryk. 2005. *Eksploatacja silników spalinowych pojazdów mechanicznych*. Piła: Wydawnictwo PWSZ.
- [28] Żurek Józef. 2009. „Wybrane metody oceny bezpieczeństwa w lotnictwie”. *Problemy eksploatacji* 4 : 61-70.
- [29] Żurek Józef. 2009. Modele oceny niezawodności obiektów technicznych. W *Materiały Konferencyjne na temat „Problematyka normalizacji, jakości i kodyfikacji w aspekcie integracji z NATO i UE”*.
- [30] Będkowski Lesław. 1992. *Elementy diagnostyki technicznej*. Warszawa: Wydawnictwo WAT.

- [31] Dąbrowski Tadeusz. 2001. *Diagnostowanie systemów antropotechnicznych w ujęciu potencjalowo-efektowym*. Warszawa: Wydawnictwo WAT.
- [32] Żółtowski Bogdan. 1996. *Podstawy diagnostyki maszyn*. Bydgoszcz: Wydawnictwo Uczelniane Akademii Techniczno -Rolniczej.

RÓWNANIA CHAPMANA–KOŁMOGOROWA DLA PEŁNEGO ZBIORU ROZRÓZNIALNYCH STANÓW DIAGNOSTYCZNYCH OBIEKTU

Paweł SZCZEPAŃSKI¹, Józef ŻUREK²

¹Wojskowa Akademia Techniczna, Wydział Mechatroniki i Lotnictwa
ul. gen. Witolda Urbanowicza 2, 00-908 Warszawa

²Instytut Techniczny Wojsk Lotniczych
ul. Księcia Bolesława 6, 01-494 Warszawa

Streszczenie. W artykule tytułowe „równania Chapmana-Kołmogorowa” są pretekstem do ukazania nieuświadomionej matematycznie prawdy o wpływie stanów diagnostycznych elementów (szeroko pojętych podmiotów) na stany diagnostyczne całego swojego zbioru, nazywanego krótko obiektem. Istotne są tu nie tylko charakterystyki niezawodnościowe poszczególnych elementów, ale przede wszystkim występujące między tymi elementami relacje niezależności, zależności i współzależności. Do opisu tych relacji posłużono się językiem teorii grafów, którego macierz osiągalności przełożono dla potrzeb wyznaczenia: liczebności i prawdopodobieństw rozróżnialnych stanów diagnostycznych obiektu, pochodnych rzeczonych prawdopodobieństw i adekwatnych tym pochodnym – intensywności przejść. Niniejszy artykuł jest kontynuacją prac wskazujących na związek właściwości pełnego zbioru rozróżnialnych stanów diagnostycznych obiektu z szeroko pojętą teorią systemów. Wcześniejsze prace odnosiły się m.in. do: ryzyka, bezpieczeństwa, entropii struktury, wiarygodności wyników sprawdzeń i – przede wszystkim – diagnostyki technicznej, tak w obszarze jej algorytmów, jak i optymalizacji. W żadnej z nich nie założono szeregowej struktury niezawodnościowej obiektu. Przykłady analiz odniesiono do wszystkich możliwych struktur konstrukcyjnych obiektu trzyelementowego. Żywi się przekonanie, że wraz z podaniem przystających do tych struktur schematów ideowych stwarza się Czytelnikowi realną możliwość praktycznej (i taniej) weryfikacji przedstawionych przemyśleń.

Słowa kluczowe: równania Chapmana–Kołmogorowa, digraf, pełny zbiór, intensywność przejścia, rozróżnialne stany diagnostyczne